

Title	Three-Dimensional Reconstruction of Fracture Surface Using Area Matching Algorithm(Physics, Processes, Instruments & Measurements)
Author(s)	Kuroda, Toshio; Ikeuchi, Kenji; Inoue, Kazuhiko; Nakade, Katsuyuki; Kitagawa, Yoshihiko
Citation	Transactions of JWRI. 30(1) P.47-P.52
Issue Date	2001-07
Text Version	publisher
URL	http://hdl.handle.net/11094/6445
DOI	
rights	本文データはCiNiiから複製したものである
Note	

Osaka University Knowledge Archive : OUKA

<https://ir.library.osaka-u.ac.jp/>

Osaka University

Three-Dimensional Reconstruction of Fracture Surface Using Area Matching Algorithm[†]

Toshio KURODA*, Kenji IKEUCHI**, Kazuhiko INOUE***, Katsuyuki NAKADE***
and Yoshihiko KITAGAWA***

Abstract

A system for the reconstruction of three-dimensional topography from stereoscopic SEM micrographs has been developed. From the relative displacement between the corresponding points measured by an area based matching procedure, the elevation of overall surface was calculated on the basis of the stereo-photographic principle, and digital elevation models (DEMs) of investigated surfaces were reconstructed on the monitor of a personal computer. The system was applied to an impact fracture surface of type 329J4L duplex stainless steel tested at 273K. The reconstructed images revealed that several cracks propagated through the ductile and brittle regions parallel to each other, keeping about 10 μ m intervals in elevation among them. The reconstruction of the cleavage fracture surface of type 444 ferritic stainless steel was made, and cleavage steps of the river pattern which the elevations are greater than the minimum elevation value can be detected and reconstructed in this system

KEY WORDS: (Scanning electron microscope) (Three-dimensional image) (Duplex stainless steel) (Fractography) (Stereo matching) (Image processing)

1. Introduction

Fractography is a technique to obtain valuable information from photographs of fracture surfaces, and it is the only measure which provides direct evidence about the fracture process inside materials¹⁾.

Scanning electron microscope (SEM) has widely been used in the field of fractography, because of the wide range of observable scale and the suitability on very rough surfaces due to the high depth of focus²⁾. However, since the analysis is based on two-dimensional information, the available results are confined in practice to the understanding of fracture morphology such as dimple or cleavage, and to the determining of the direction of macro crack propagation.

It is desirable to consider the information associated with three-dimensional morphology of fracture surfaces for more detailed analysis. An analysis technique using a stereoscopic viewer has been performed.

The operator can combine two stereo images into a three-dimensional landscape in his brain, but the information obtained depends on the operator's subjectivity and has not been yet quantitative. On the other hand, the

measuring parallax between two stereo images is a suitable technique for quantitative analysis of fracture surfaces. The elevation of inspected areas can be calculated on the basis of the stereo-photography principle. Since at first this procedure was done manually^{3),4)}, the analysis was time-consuming and was relatively inaccurate, because of human errors. It was impossible to acquire an overall profile of fracture surfaces.

In 1980s the process of parallax measurement was automated using digital image processing technology which rapidly developed with the progress in the performance of computers. The topography of various kinds of fracture surfaces was visualized through a monitor. However, these attempts were performed on super computers or dedicated purpose workstations^{5), 6)}.

In this study we developed an automatic reconstruction system for fractographic analysis which works on general personal computers and displays three-dimensional reconstruction images of the digital elevation model (DEM) from the stereoscopic SEM micrographs of investigated fracture surfaces. There are few reports dealing with the relation between materials microstructure and topography of fracture surfaces; we fo-

[†] Received on May 31, 2001

* Associate Professor

** Professor

*** Graduate student

Transactions of JWRI is published by Joining and Welding Research Institute of Osaka University, Ibaraki, Osaka 567-0047, Japan.

Three-Dimensional Reconstruction of Fracture Surface

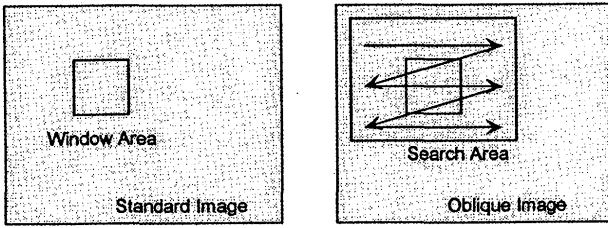


Fig. 1 Schematic illustration of the searching the corresponding points.

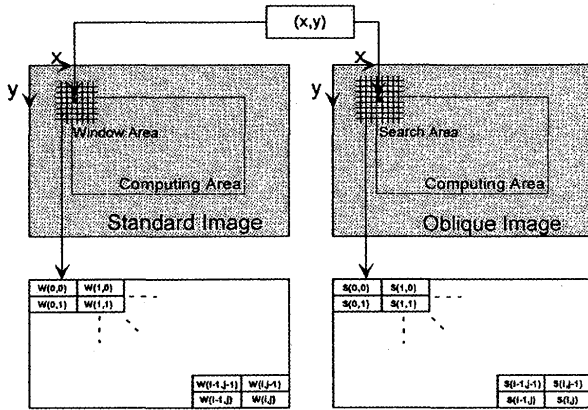


Fig. 2 Setting window area in standard image and search area in oblique image.

cus on it by applying the developed system to fracture surfaces of stainless steels.

2. Reconstruction Procedure for Three-dimensional Topography

2.1 Searching for Corresponding Points to Measure Parallax

Stereoscopic micrographs are obtained from SEM images of specimens tilted in two different angles to each other. We decided to adopt 4° or 8° as the tilting angle between two images. The micrographs obtained are digitized using an image scanner with 256 gray levels. And then an area-based matching called template matching is carried out to find corresponding points from two surface projections.

A schematic representation for the template matching is shown in Fig. 1. A size of "window area" is placed on the first stereo image (called "standard image"). On the second stereo image ("oblique image") a window of the same dimension is moved around within a search area to find the position where the two windows show the maximum correspondence⁷. SSDA⁸ (Sequential Similarity Detection Algorithm) and MCC⁹ (Mutual Correlation Coefficient) were used for the estimation.

SSDA is a fast algorithm for the template matching which calculates the difference between two windows by subtracting gray levels of each pixel in the windows and the position where the sum of the absolute differences

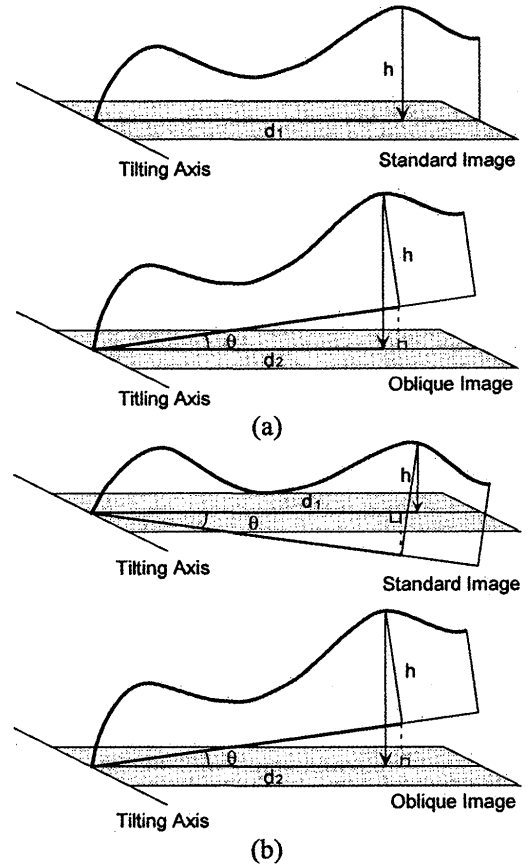


Fig. 3 Schematic illustration of topography along cross section: (a) Using 0 degree-tilted image as standard image and $+\theta$ degree-tilted image as oblique image and (b) Using $-\theta$ degree-tilted image as standard image and $+\theta$ degree-tilted image as oblique image.

shows the minimum is decided to be the maximum correspondence. In Fig. 2 the difference of the two windows is calculated as follows:

$$E(m, n) = \sum_{j=0}^{J-1} \sum_{i=0}^{I-1} |W(i, j) - S(m+i, n+j)|, \quad (1)$$

where $W(i, j)$ and $S(m+i, n+j)$ are the gray levels of each pixel in the windows placed on the standard image and the oblique image respectively. In the implementation the calculation is terminated before all the pairs are tested when $E(m, n)$ exceeds a threshold value to reduce redundancy.

MCC detects the position of the maximum correspondence by calculating cross-correlation of the two windows. In Fig. 2 the cross-correlation coefficient of the two windows is calculated as follows:

$$R(m, n) = \frac{\sum_{j=0}^{J-1} \sum_{i=0}^{I-1} (W(i, j) - \bar{W})(S(m+i, n+j) - \bar{S}(m, n))}{\sqrt{\sum_{j=0}^{J-1} \sum_{i=0}^{I-1} (W(i, j) - \bar{W})^2} \sqrt{\sum_{j=0}^{J-1} \sum_{i=0}^{I-1} (S(m+i, n+j) - \bar{S}(m, n))^2}}$$

$$R(m,n) = \frac{\sum_{j=0}^{J-1} \sum_{i=0}^{I-1} (W(i,j)S(i+m,j+n) - IJ\bar{W}\bar{S}(m,n))}{\sqrt{\sum_{j=0}^{J-1} \sum_{i=0}^{I-1} (W(i,j)^2 - IJ\bar{W}^2)} \sqrt{\sum_{j=0}^{J-1} \sum_{i=0}^{I-1} (S(m+i,n+j)^2 - IJ\bar{S}(m,n)^2)}} \quad (2)$$

where \bar{W} and $\bar{S}(m,n)$ are the average gray levels of each window which are represented by

$$\bar{W} = \frac{1}{IJ} \sum_{j=0}^{J-1} \sum_{i=0}^{I-1} W(i,j), \quad \bar{S}(m,n) = \frac{1}{IJ} \sum_{j=0}^{J-1} \sum_{i=0}^{I-1} S(m+i,n+j). \quad (3)$$

The higher $R(m,n)$ indicates the higher correspondence. Then the centers of the two windows are decided to be corresponding points and the elevation can be obtained. When the tilt angle is 0° and θ° (Fig. 3(a)), the elevation is calculated by following equation:

$$h = \frac{d_1}{\tan \theta} - \frac{d_2}{\sin \theta}, \quad (4)$$

where d_1 and d_2 are distances from a standard point to the

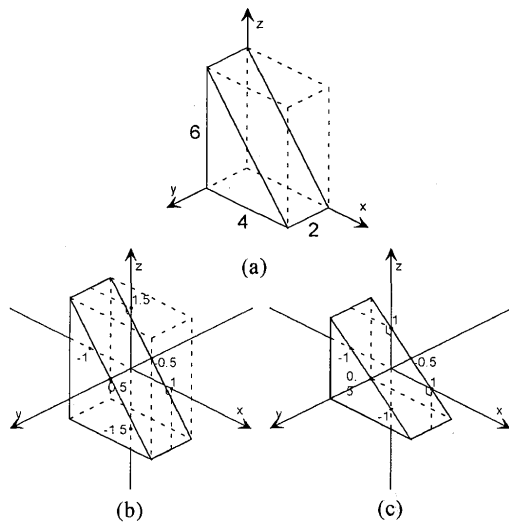


Fig. 4 Method of transforming coordinates.

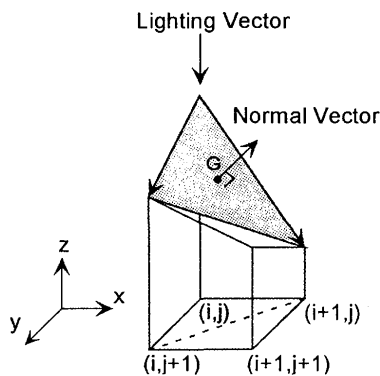


Fig. 5 Constructing three-dimensional face.

corresponding points, and when the tilt angle is $\pm\theta^\circ$ (Fig. 3(b)), the equation is written as

$$h = \frac{d_1 - d_2}{2\sin \theta}. \quad (5)$$

2.2 Displaying Digital Elevation Models

The elevation data obtained are outputted as a CSV (Comma Separated Values) format file to display a DEM on a monitor via OpenGL; the programming library for two-dimensional and three-dimensional computer graphics¹⁰.

First of all, three-dimensional coordinates of DEMs are manipulated so that all the values range from -1 to 1 to coincide with the coordinate system of OpenGL. At first, the scaling rates of the coordinates are determined based on the range of x and y values. After that, the z axis is scaled down further only when the values exceed the range of -1 to 1 , which means the scaling rates of x - y axis and z axis may be different depending on the shape of the surface. An example with actual values is represented in Fig. 4.

Figure 5 is a schematic representation of the way of

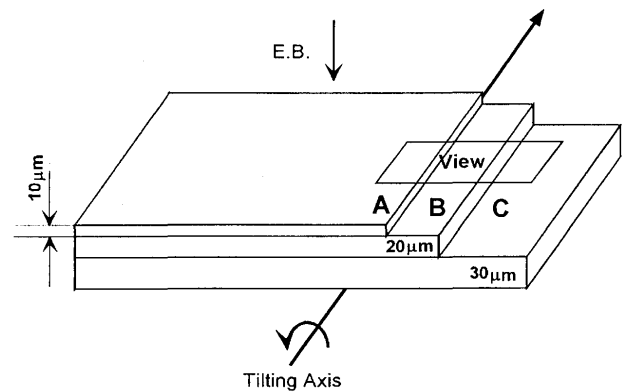


Fig. 6 Schematic illustration of specimen made of feeler gauges.

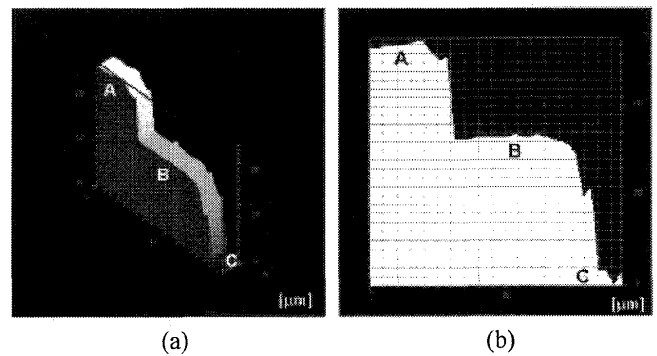


Fig. 7 Three-dimensional reconstruction of the feeler gauges: (a): Three-dimensional image, (b): Cross-sectional profile of two-dimensional image.

Three-Dimensional Reconstruction of Fracture Surface

making surfaces from the points of three-dimensional coordinates and lighting them. DEMs consist of sets of triangles, the vertices of which are taken from contiguous three points. The brightness of each triangle is determined from the angle between its normal vector and a lighting vector. The surface becomes brighter as the angle gets close to 90°. These programs were developed on “Microsoft Visual C++ 6.0” and designed to run under Windows platforms.

3. Results and Discussion

3.1 Confirmation of accuracy on known geometry

To confirm the accuracy of the system, three-dimensional reconstruction of a feeler gauge, the thickness of which is known was performed. The thickness of the feeler gauge used is 10 μm , 20 μm and 30 μm . As shown in Fig. 6, three gauges overlapped each other with no seams among them and the observation was conducted at the steps of 10 μm and 20 μm . The reconstructed DEM and its cross sectional profile are shown in Fig. 7(a) and Fig. 7(b). The specified values of the gauges in thickness are $10 \pm 3 \mu\text{m}$ and $20 \pm 3 \mu\text{m}$, and a micrometer (Mitutoyo Digimatic Outside Micrometer 293) was used to measure the actual values. Twenty points were measured for each

points were measured for each gauge. For the gauge of 10 μm , the values measured were in the range of 10 to 11 μm , and for the gauge of 20 μm , the micrometer indicated the thickness of 18 to 20 μm . From the cross sectional profiles taken from the DEM the thickness was measured as 10 to 11 μm and 16 to 17 μm respectively, which is considered to be within reasonable values.

3.2 Fracture surface of duplex stainless steel

Figure 8 shows a pair of stereographs of Charpy impact fracture surface for type 329J4L duplex stainless steel. The test was performed at 273K. The left photograph represents a standard image (-4°) and right one represents an oblique image (+4°). The fracture surface can appear as a three-dimensional image when the stereographs are observed with a stereoscope.

The fracture surface consists of ductile regions and brittle regions. In the ductile regions marked as A and B, dimple patterns with inclusions are observed. Brittle fracture is considered to have occurred in the regions marked as C and D.

Figure 9 represents the SEM micrograph and the DEM reconstructed where the viewpoint is located right above the surface for comparison. The white edges ob-

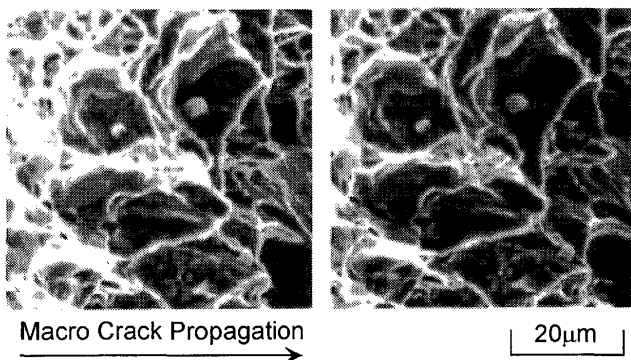


Fig. 8 SEM stereographs of the fracture surface of type 329J4L duplex stainless steel from a Charpy impact test at 273K.

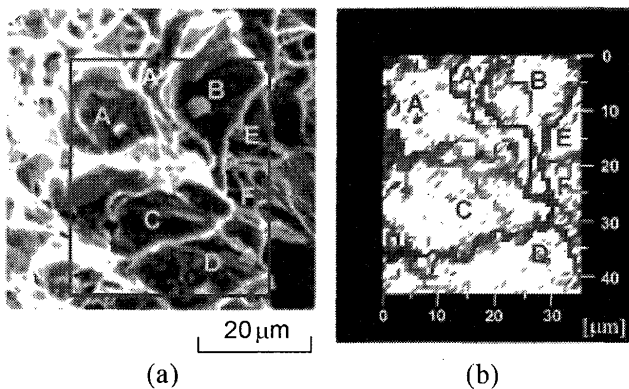
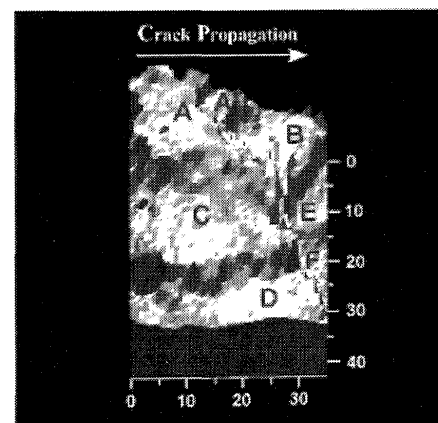
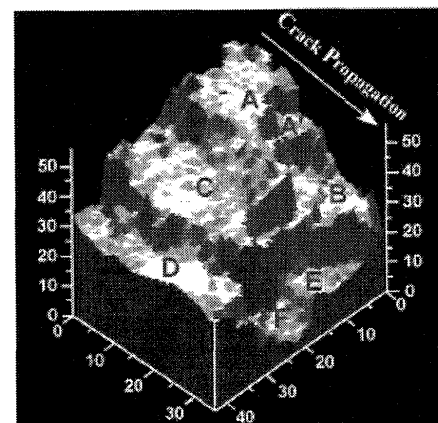


Fig. 9 Comparison of Fracture surface by SEM (a) and three-dimensional reconstruction image (b).



(a)



(b)

Fig. 10 Three-dimensional reconstruction images of the fracture surface.

Macro Crack Propagation



Fig. 11 SEM micrograph of fracture surface of type 444 ferritic stainless steel from Charpy impact test at 77K (standard image).

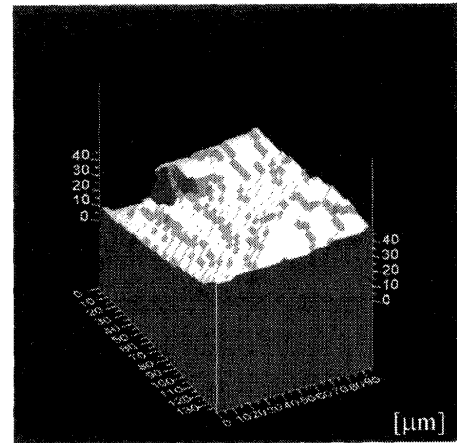
served in the micrograph appear as the black lines in the DEM for the slanted steps existing there. The location of these lines shows a good match to those of the micrograph.

Figure 10(a) shows a view from a different location. A step can be seen between the region C and D in this viewpoint. From the viewpoint in Fig. 10(b), several steps can be observed quantitatively. The DEM reveals that several cracks have propagated through the ductile and brittle regions parallel to each other, keeping about 10 μm intervals in elevation among them. This is considered to relate to the distribution of austenite grains.

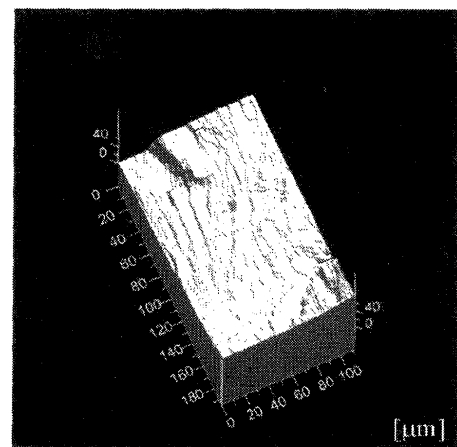
By observing DEMs from several viewpoints as shown in Fig. 10, we can obtain advanced information (three-dimensional morphology with quantitative values) which is impossible to obtain in the observation of SEM micrographs.

3.3 Cleavage fracture surface of ferritic stainless steel

The system has a minimum value with respect to surface geometry which is detectable from digital stereo images. The value is determined numerically from the conditions of stereo-photographs. The elevation when parallax is equivalent to one pixel is the minimum eleva-



(a)



(b)

Fig. 12 Three-dimensional images from the SEM micrograph showing cleavage steps. (a) Resolution of 150 dpi and (b) Resolution of 300 dpi.

tion value. It can be written as

$$h_c = \frac{25.4}{M \cdot R \sin \Delta \theta} \text{ (mm)}, \quad (6)$$

where h_c is the minimum elevation, M and R are the magnification and resolution of the image respectively and $\Delta \theta$ is the tilting angle between two images. Elevations are represented by integral multiples of h_c ; therefore this value is identical with the vertical resolution of DEMs.

Figure 11 shows a SEM micrograph of the fracture surface of type 444 ferritic stainless steel tested at 77K. The cleavage fracture showing river pattern can be seen in the SEM micrograph.

Figure 12 shows three-dimensional reconstructed images of various scanning resolutions was performed for the fracture surface of type 444 ferritic stainless steel. The resolutions adapted here are 150 and 300 dpi; the corresponding minimum elevation values (h_c) are calcu-

Three-Dimensional Reconstruction of Fracture Surface

lated from Eq. (6) as $2.17 \mu\text{m}$ and $1.08 \mu\text{m}$ respectively with the conditions of magnification of 560 and θ of $\pm 4^\circ$.

It is apparent that cleavage steps which the elevations are greater than the minimum elevation value can be detected and reconstructed in this system.

4. Conclusion

- (1) A new system for the reconstruction of the three-dimensional topography from stereoscopic SEM micrographs has been developed. From the relative displacement between the corresponding points measured by an area-based matching procedure, the elevation of the overall surface is calculated on the basis of the stereo-photography principle. Digital elevation models (DEMs) of investigated surfaces were reconstructed on a monitor of a personal computer.
- (2) The system was applied to the ductile fracture surfaces of duplex stainless steel. The reconstructed images revealed that several cracks propagated through the ductile and brittle regions parallel to each other, keeping about $10 \mu\text{m}$ intervals in elevation among them.
- (3) An equation determining the accuracy of three-dimensional images from the stereo-photographs conditions has been introduced. The reconstruction of the cleavage fracture surface of type 444 ferritic stainless steel was performed, and cleavage steps of the river pattern which the elevations are greater

than the minimum elevation value can be detected and reconstructed in this system.

References

- 1) JSMS Committee on Fractography, Fractography, Maruzen, Tokyo (2000) (in Japanese).
- 2) The Society of Japan Electron Microscopy, Scanning Electron Microscopy, Kyo-ritu-Shuppan, Tokyo (1976) (in Japanese)
- 3) A.J.Krasowsky and V.A.Stepanenko, International Journal of Fracture, Vol.15, No.3 (1979), 203
- 4) T. Kobayashi, G. R. Irwin and X. J. Zhang, ASTM STP 827, J. J. Mecholsky Jr. and S. R. Powell Jr. Eds., American Society for Testing and Materials (1984), 234
- 5) K. Komai and J. Kikuchi, J. Soc. Mat. Sci., Japan, 34 (1984), 648 (in Japanese)
- 6) K. Komai and M. Noguchi, J. Iron and Steel Inst. Japan, 72 (1986), 2125 (in Japanese).
- 7) K. Komai and M. Noguchi, Fractography, Current Japanese Materials Research Vol.6, R. Koterazawa, R. Ebara and S. Nishida Eds., ELSEVIER APPLIED SCIENCE, London and New York (1990), 161
- 8) D. I. Barnea and H. F. Silverman, IEEE Transaction on Computers, Vol.c-21, No.2 (1972), 179
- 9) J. A. Leese, C. S. Novak and B. B. Clark, J. Applied Meteorology, Vol.10 (1971), 118
- 10) C. Walnum, 3-D Graphics Programming with OpenGL, Prentice Hall, Japan (1996) (in Japanese)